J. Phys. B: At. Mol. Opt. Phys. **33** (2000) 4747–4758. Printed in the UK PII: S0953-4075(00)50810-4

Cross sections for the reaction $H^+ + H_2$ (v = 0–14) $\rightarrow H + H_2^+$ at low collision energies

Akira Ichihara†, Osamu Iwamoto† and R K Janev‡

† Nuclear Data Center, Japan Atomic Energy Research Institute, Tokai-mura, Ibaraki, 319-1195, Japan

‡ National Institute for Fusion Science, Oroshi-cho, Toki, Gifu, 509-5292, Japan

E-mail: ichihara@ndc.tokai.jaeri.go.jp

Received 18 May 2000, in final form 25 July 2000

Abstract. Cross sections for the reaction $H^+ + H_2 \rightarrow H + H_2^+$ have been calculated in the centre-of-mass collision energy range of $E_{cm} \leqslant 20$ eV by using the trajectory-surface-hopping method. The vibrational quantum number of the reactant H_2 has been taken to be in the range $0 \leqslant v \leqslant 14$, and the effect of v on H_2^+ production has been investigated. The results show that H_2^+ production increases rapidly as v increases up to $v = 5, 6$, and then decreases with further increase of v. The Maxwellian-averaged rate coefficients, which are expressed as functions of the plasma and H_2 temperatures (T, E), have been estimated from the calculated cross sections in the range $0.1 \leqslant T$, $E \leqslant 5.0$ eV.

1. Introduction

The H_3^+ system has been attracting the interest of both experimentalists and theorists for more than two decades (see, e.g., [1–9]). Ion–molecule reactions occurring in the H_3^+ system and its isotopic variants provide an excellent opportunity for direct comparison between experiment and theory [3, 5, 6]. Accurate knowledge of the cross sections for these reactions is important for the analysis of plasma behaviour in divertors of toroidal fusion devices [7, 8], where the existence of neutral atoms and molecules is supported by low plasma temperatures ($\leqslant$10–20 eV). In particular, the ion-conversion reaction $H^+ + H_2 \rightarrow H + H_2^+$ is expected to play a crucial role in the volume recombination of divertor plasmas at temperatures of 0.3–3 eV [9, 10].

Earlier studies of collision processes in the $H^+ + H_2$ system were mainly confined to the vibrationally unexcited molecules. We have previously calculated the ion production cross sections in the $H^+ + H_2$ collision system and its isotopic variants within the framework of the conventional trajectory-surface-hopping (TSH) model [11, 12]†. It has been shown that the calculated cross sections for the H^++D_2 ($v = 0$), D^++H_2 ($v = 0$) and D^++D_2 ($v = 0$) systems, where v is the vibrational quantum number, are in good agreement with the experimental cross sections in the centre-of-mass collision energy range of $2.5 \leqslant E_{cm} \leqslant 8.0$ eV [11, 13, 14].

Collision processes in this system with vibrationally and rotationally excited H_2 in the entrance channel also have significant theoretical and practical importance. Excitation of vibrational states of H_2 in divertor plasmas is expected due to the effectiveness of several

† It should be noted that the square root of the hopping coefficient E_c is given as a function of ΔE_0 in figure 1 of [11].

0953-4075/00/214747+12$30.00 © 2000 IOP Publishing Ltd

collision processes in the collision energy range corresponding to the temperatures of these plasmas (0.3–20 eV): $v - v'$ ($v' > v$) processes by electron and (particularly) proton impact, electron impact excitation of excited electron (singlet) molecular states that are radiatively coupled with the 1 Σ_g^+ ground molecular state followed by radiative decay to the ground state in higher vibrational states, electron impact excitation of the resonant states of H_2^- ion followed by its autodetachment decay to the vibrationally excited H_2 states, etc. Vibrationally excited H_2 molecules may also be released from the divertor walls following the H_2^+ charge exchange on the wall surfaces and associative formation of H_2 on divertor wall surfaces upon low-energy proton or H impact.

With increasing internal energy of the H_2 molecule in its initial state, the collision dynamics change significantly (transition from endo- to exothermic reaction conditions). The experimental study of state-selective processes in the H_3^+ system is rather difficult and a theoretical approach based on the TSH model seems to be at present the most practical approach to 'hot' H_3^+ dynamics, provided the collision energy is significantly high [11, 15].

In the present paper, we shall study the reaction $H^+ + H_2$ ($v = 0$ to 14, $j = 1$) $\rightarrow H + H_2^+$ in the centre-of-mass collision energy range of $E_{cm} \leqslant 20.0$ eV, where the initial rotational quantum number of reactant H_2 is fixed as $j = 1$. We shall investigate, in particular, the v dependence of the cross section. We shall also calculate the Maxwellian-averaged rate coefficients from the calculated cross sections in the plasma (T) and H_2 (E) temperature range of 0.1–5.0 eV, which are of interest in the current fusion divertor plasma research [8–10].

2. Details of the calculation

The method adopted for the cross section calculations is based on the trajectory-surface-hopping method of Tully and Preston [16]. The details of the computational method are described in [11, 16–18]. Rate coefficients have been evaluated from the calculated cross sections by using the formula given in [19].

In the TSH model employed, the surface hop takes place on the point of the avoided crossing of two potential energy surfaces (PESs) of H_3^+ in the $^1A'$ electronic states. Thus the surface hop is treated as a Landau–Zener-type transition [20–22]. We assumed that the avoided crossing appears in the region where the distance r between two protons is 2.5 a_0 (where a_0 is the Bohr radius defined by 1 $a_0 = 0.529\,177 \times 10^{-8}$ cm) and the distance R from the midpoint of the proton pair to the third proton is greater than 5.0 a_0. The probability of surface hopping (the LZ transition probability) is calculated when the trajectory passes the avoided crossing point. We employed the formula derived by Zhu and Nakamura [23, 24] to evaluate the hopping probability†.

In the trajectory calculation, the incoming proton was initially separated at 15 a_0 from the hydrogen molecule. The Hamiltonian equations of motion were integrated with time steps in the range 2–3 $\times 10^{-17}$ s. The integration was terminated when the products reached a separation of $R \geqslant 15\ a_0$ and two of the three internuclear distances were $r_{bc}, r_{ca} \geqslant 10\ a_0$. Then, the two more closely spaced protons were treated as a diatomic product. The internal energy of the diatomic product was calculated at the terminal point of each trajectory and the dissociation was considered to happen if the turning point for the vibration of the diatomic molecules could not be found within $r < 10\ a_0$. Some trajectories remained trapped in the reaction region even after 1.2×10^{-12} s of flight time for low collision energies. The number of

† The hopping probability was calculated using equation (3.7) of [24] with parameters defined by equations (3.3)–(3.6) and (3.10).

Table 1. Comparison of cross sections calculated from the *ab initio* and the DIM potential energy surfaces.

	Cross section (σ, $\Delta\sigma$ in 10^{-16} cm^2)				
	Ab initio		DIM		
E_{cm} (eV)	σ	$\Delta\sigma$	σ	$\Delta\sigma$	σ(DIM)/σ(*ab initio*)
$H^+ + H_2(v = 0, j = 1) \rightarrow H + H_2^+$					
2.0	0.014	0.003	0.009	0.002	0.643
3.0	0.656	0.024	0.611	0.021	0.931
4.0	0.821	0.024	0.738	0.021	0.899
6.0	1.167	0.025	0.997	0.022	0.854
8.0	0.954	0.022	0.837	0.019	0.877
12.0	0.784	0.020	0.702	0.017	0.895
20.0	0.605	0.017	0.591	0.014	0.977
($v = 1, j = 1$)					
2.0	0.525	0.024	0.542	0.025	1.032
3.0	0.907	0.027	0.909	0.026	1.002
4.0	1.474	0.032	1.196	0.027	0.811
6.0	1.230	0.027	1.082	0.025	0.880
8.0	1.072	0.026	1.069	0.025	0.997
12.0	1.382	0.038	1.359	0.038	0.983
20.0	2.383	0.056	2.140	0.050	0.898
($v = 3, j = 1$)					
1.0	1.820	0.059	1.445	0.052	0.794
2.0	4.283	0.088	3.997	0.084	0.933
4.0	3.348	0.066	3.164	0.067	0.945
6.0	3.651	0.075	2.887	0.065	0.791
8.0	5.529	0.095	4.305	0.084	0.779
12.0	9.139	0.122	6.989	0.105	0.765
20.0	11.494	0.134	9.214	0.118	0.802
($v = 5, j = 1$)					
1.0	32.284	0.262	33.222	0.273	1.029
2.0	36.702	0.255	36.031	0.265	0.982
4.0	35.724	0.251	34.467	0.258	0.965
6.0	31.726	0.244	30.336	0.252	0.956
8.0	31.839	0.239	29.495	0.247	0.926
12.0	35.198	0.228	33.267	0.239	0.945
20.0	39.455	0.209	36.960	0.219	0.937
($v = 6, j = 1$)					
1.0	33.280	0.253	32.228	0.263	0.968
2.0	37.684	0.240	38.072	0.249	1.010
4.0	33.322	0.240	32.835	0.246	0.985
6.0	31.319	0.232	29.628	0.239	0.946
8.0	32.102	0.223	30.727	0.230	0.957
12.0	35.982	0.205	34.986	0.214	0.972
20.0	38.806	0.186	37.403	0.193	0.964

such trajectories never exceeded 1% of all trajectories for every (v, E_{cm}) and these trajectories were eliminated from the final product assignment.

200 trajectories were run in the impact parameter interval $[b_{i-1}, b_i]$ for each $i = 1, 2, \ldots,$ max, where $b_0 = 0.0\,a_0$ and $\Delta b = b_i - b_{i-1}$ was fixed at $0.076\,a_0$ (0.04×10^{-8} cm). The impact parameter b in $[b_{i-1}, b_i]$ was selected to have a uniform distribution between b_{i-1}^2

and b_i^2. The calculations were continued until it was confirmed that 4000 trajectories in the interval $[b_{\max}, b_{\max}+20\Delta b]$ did not exhibit any reaction: charge transfer, nuclear rearrangement or dissociation. To terminate the calculation, the hopping probability was set to be unity if $P > 0.99$. Under the constraint, $b_{\max}$ obtained was less than 11 a_0 for every (v, $E_{\rm cm}$). Then, the cross section and associated error (σ, $\Delta\sigma$) were evaluated from a set of trajectories in $[0, b_{\max}]$ [18].

In the present calculation, the three-dimensional *ab initio* potential energy surfaces [25] have been used for $v \leqslant 6$, and the diatomics-in-molecules (DIM) model potentials [26] have been used for $v \geqslant 7$. The *ab initio* PESs have been constructed from potential energies calculated at 701 spatial geometries by the full configuration-interaction (full-CI) method with an [8s6p2d1f] Gaussian-type basis set [25]. Although the *ab initio* PESs are more theoretical than DIM-PESs, the numerical uncertainty appears in the interpolation of the *ab initio* PESs in the region where the distance between protons is larger than 4.0 a_0, owing to the lack of calculated energy points. Since DIM-PESs are given by the analytical formulae in the whole area of trajectory calculation, DIM-PESs have been employed for high-v states. Input parameters of DIM-PESs are taken to be the same as those used by Schlier *et al* [14]

The cross sections calculated with DIM-PESs for $v = 0$, 1, 3, 5 and 6 have been compared with those with the *ab initio* PESs to examine the applicability of DIM-PESs. Table 1 shows the results for several collision energies. It can be seen from table 1 that the difference of cross sections calculated from the *ab initio* and DIM-PESs is less than 20% for every (v, $E_{\rm cm}$) if the numerical error is taken into account. In particular, the difference is less than 5% for $v = 5$ and 6. From these results we assumed that the cross sections are not sensitive to the difference between the *ab initio* and DIM-PESs, and thus we employed DIM-PESs for $v \geqslant 7$.

To investigate the validity of the TSH model employed, calculated cross sections for $v = 0$ have been compared with existing experimental data. In our previous calculations for $D^+ + D_2$ and $H^+ + D_2$ in $2.5 \leqslant E_{\rm cm} \leqslant 8.0$ eV, the calculated cross sections for charge transfer are larger than the experiments of Schlier *et al* [14] and Ochs and Teloy [13] for $E_{\rm cm} \geqslant 5.0$ eV, and the deviation increases with increasing $E_{\rm cm}$ [11]. However, if the experimental uncertainties, which are 10% for $D^+ + D_2$ and 20% for $H^+ + D_2$, are taken into account and experimental cross sections are multiplied by factor of 1.1 or 1.2, the difference between the experiments and the TSH calculations is reduced to about 10% for 8.0 eV. The TSH cross sections for the $H^+ + H_2$ system have also been compared with the experiment and quantum mechanical calculation. From the experimental cross section $0.334 \pm 0.087 \times 10^{-16}$ cm^2 at $E_{\rm cm} = 42$ eV measured by Gealy and Van Zyl [27], the experimental value for $E_{\rm cm} = 20$ eV is estimated to be $0.70 \pm 0.18 \times 10^{-16}$ cm^2, assuming that the charge transfer cross section decreases as $E_{\rm cm}^{-1}$. The corresponding TSH results from the *ab initio* and DIM-PESs are $0.605 \pm 0.017 \times 10^{-16}$ and $0.591 \pm 0.014 \times 10^{-16}$ cm^2, respectively, which are in quantitative agreement with the experimental value. The quantum mechanical calculation has been carried out by Baer at 20 eV with the infinite-order sudden approximation (IOSA) on DIM-PESs [28], and the cross section was evaluated to be 1.1×10^{-16} cm^2. The difference between our result and the IOSA result is within a factor of two. From the above results we expected that using the TSH model was appropriate for estimating the cross section within the range $E_{\rm cm} \leqslant 20$ eV.

3. Results and discussion

Figure 1 shows the cross sections for the reaction $H^+ + H_2$ ($v = 0$–14) $\rightarrow H + H_2^+$. It can be seen from figure 1 that H_2^+ production increases rapidly as v increases up to $v = 5$ and then decreases gradually for $v \geqslant 7$. In this reaction, H_2^+ is produced by pure charge (or electron)

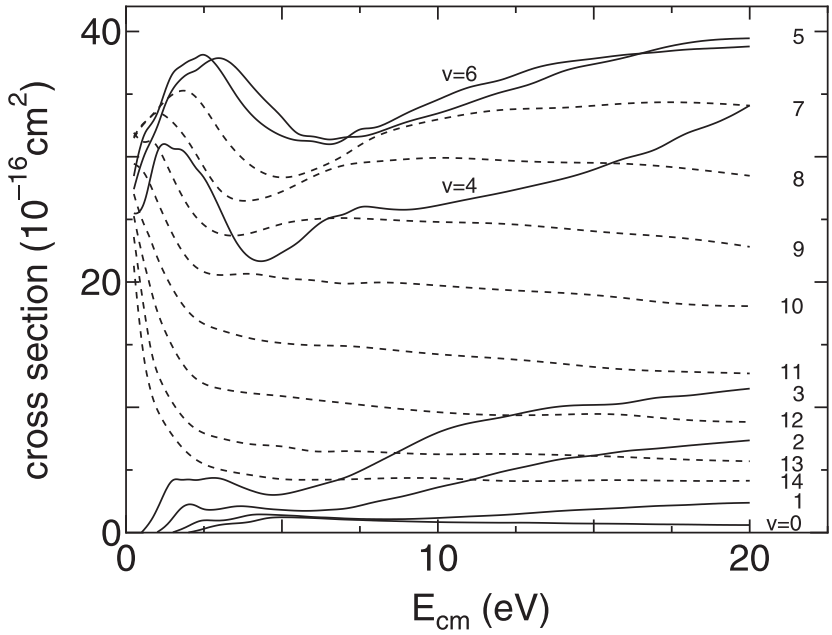

Figure 1. The TSH cross sections for the reaction $H^+ + H_2$ ($v = 0$–14, $j = 1$) $\rightarrow$ $H + H_2^+$. The cross sections are given as a function of the centre-of-mass collision energy E_{cm}.

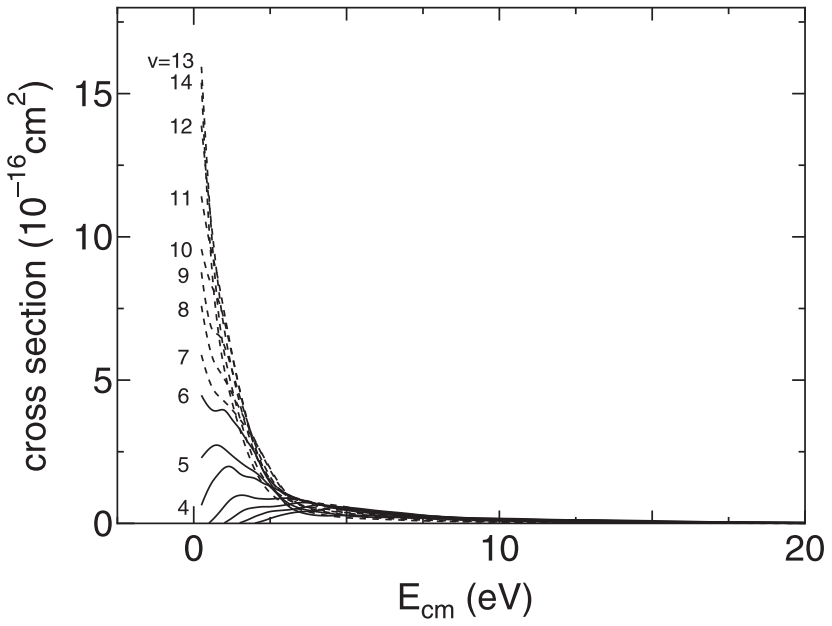

Figure 2. The contribution of the charge transfer reaction with proton rearrangement to H_2^+ production from the $H^+ + H_2$ ($v = 0$–14, $j = 1$) collisions. The TSH cross sections are given as a function of the centre-of-mass collision energy E_{cm}.

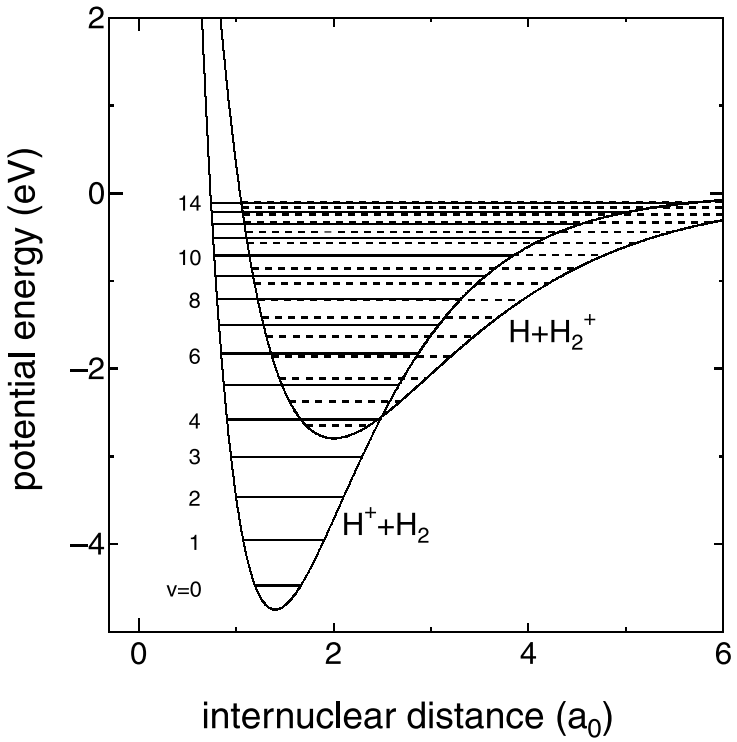

Figure 3. Section of the DIM-potential energy surfaces at $R = 10.0\ a_0$ in an isosceles triangle geometry. R is the distance between a proton and a hydrogen molecule. The potential curves are given as a function of the internuclear distance r between two protons. In the figure, the vibrational energy levels of H_2 and H_2^+ are shown by the full and broken lines, respectively.

transfer and by charge transfer with proton exchange. Figure 2 shows the contribution of the latter reaction to H_2^+ production. We can see from figures 1 and 2 that the H_2^+ ions are produced mainly by pure charge transfer (electron capture).

The enhancement of H_2^+ production by pure charge transfer for $0 \leqslant v \leqslant 4$ can be explained from the features of PESs employed. Figure 3 shows the section of the DIM-PESs at $R = 10.0\ a_0$ in an isosceles triangle geometry, where R is the distance between H^+ and H_2. PESs are given as a function of the internuclear distance r of H_2. It can be seen from figure 3 that the avoided crossing of two PESs appears at $r = 2.5\ a_0$, where the electronic structure of PES in the ground state changes from $H^+ + H_2$ to $H + H_2^+$ drastically. It is known that the avoided crossing appears in the region ($r \approx 2.5\ a_0$, $R > 5.0\ a_0$) in the three-dimensional PESs [25, 29], and thus the seam of avoided crossing appears perpendicular to r and parallel to R. In figure 3 H_2^+ production is induced when a trajectory running on the ground-state PES reaches the avoided crossing point, since the choice of PES (upper or lower) to use for the subsequent trajectory calculation is determined at this point. From figure 3, H_2 in the $v > 4$ state can take the value $r = 2.5\ a_0$ at which the avoided crossing takes place, so that H_2^+ production becomes possible if H_2 is excited into the $v > 4$ vibrational state†. Thus, if the reactant H_2 is

† The turning point of H_2 vibration in the $v = 4$ state appears at the avoided crossing point in PESs. In this case the vibration velocity is almost zero at the point of avoided crossing, so that the hopping probability dose not converge to unity, even if the trajectory is in the asymptotic region. Thus, the TSH calculation does not converge with a finite value of the maximum impact parameter. To avoid this problem, we shifted the $v = 4$ level to 0.01 eV upward artificially.

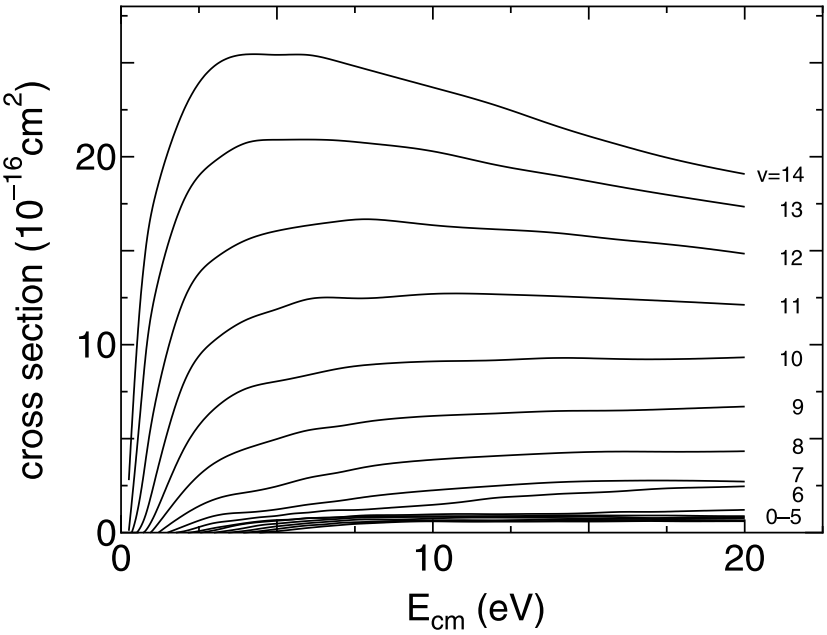

Figure 4. TSH cross sections for the reaction $H^+ + H_2$ ($v = 0$–14, $j = 1$) $\rightarrow$ $H^+ + H + H$. The cross sections are given as a function of the centre-of-mass collision energy E_{cm}.

in the vibrational excited state in advance, further vibrational excitation into the $v > 4$ state is brought about easily by collision with H^+. Therefore, H_2^+ production is enhanced remarkably with increasing v for $v \leqslant 4$.

In figure 3 the vibration amplitude for the $v = 5$ states is larger than 2.5 a_0. Thus, the increase of H_2^+ production cross sections between $v = 4$ and 5 may be due to increasing charge transfer which does not require internal excitation of H_2. This reaction can take place when a proton passes through H_2 with a large impact parameter, so that the cross section changes appreciably between $v = 4$ and 5.

In the TSH model employed, whether a surface hop takes place or not is determined by the hopping probability. The hopping probability P can be expressed as $P = \exp(-C/u)$, where C is the coefficient derived from the shape of PESs, and u is the component of trajectory velocity perpendicular to the avoided crossing seam measured from midway between two PESs at the avoided crossing. Therefore, the magnitude of the charge transfer cross section depends strongly on the density of trajectories on the avoided crossing seams and the distribution of u. It appears that these two factors maximize the reaction probability at $v = 5$ and 6, leading to the maximization of the cross section $\sigma(v)$ at these values.

In figure 1 the H_2^+ production cross section decreases gradually with increasing v for $v \geqslant 7$. The decrease is attributed to increasing dissociation. Figure 4 shows the cross sections for the dissociation $H^+ + H_2$ ($v = 0$–14) $\rightarrow$ $H^+ + H + H$. As the H–H bond weakens with increasing v, dissociation becomes probable for a high-v state. The decrease of the H_2^+ production cross section may also be due to the velocity u dependence of the hopping probability P. P tends to unity as u increases. If P is unity, electronic transition between $H^+ + H_2$ and $H + H_2^+$ does not happen in figure 3. As the trajectories have large vibrational velocities at the avoided crossing point for a high-v state, H_2^+ production may be reduced for a high-v state. Therefore,

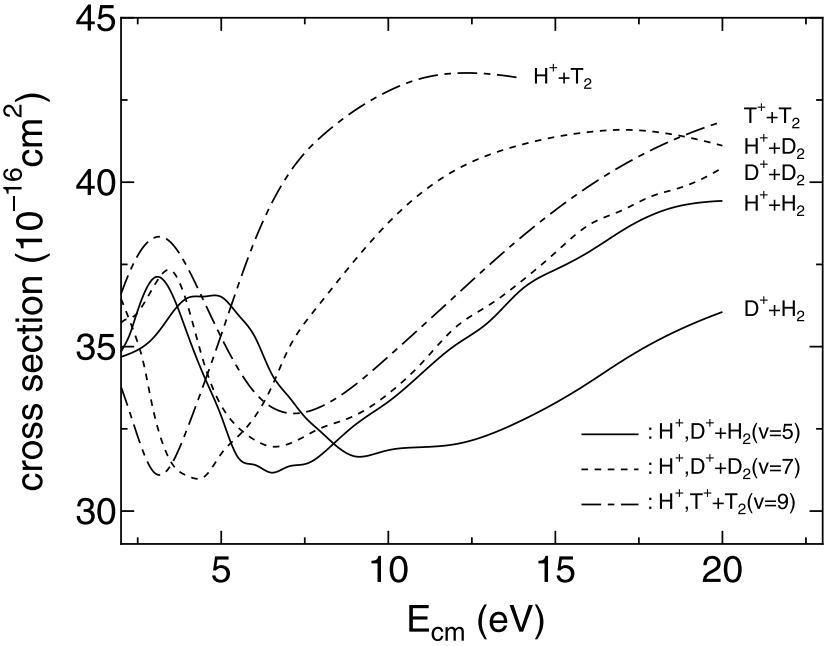

Figure 5. The E_{cm} dependence of the TSH cross sections for pure charge transfer. Full curves, H^+, $D^+ + H_2$ ($v = 5$, $j = 1$); broken curves, H^+, $D^+ + D_2$ ($v = 7$, $j = 1$); chain curves, H^+, $T^+ + T_2$ ($v = 9$, $j = 1$).

the decrease in H_2^+ production is thought to come from increasing dissociation and from the features of the hopping probability.

In figure 2 H_2^+ production with proton exchange is appreciable for E_{cm} below 2 eV. At low collision energies, many H_2^+ ions may be produced via the formation of a long-lived H_3^+ intermediate, because PES in the ground state has a deep well for the stable H_3^+ molecular ion. H_3^+ has an equilibrium geometry at an equilateral triangle of side 1.65 a_0 and the equilibrium energy is 4.6 eV lower than the H_2 equilibrium energy [25]. In our calculation, a trajectory starting from the asymptotic region of the ground-state PES is trapped around the well and the proton exchange is induced there. After proton exchange, H_2^+ production is induced if the trajectory can reach the avoided crossing seam. Since the number of trajectories trapped in the potential well increases with decreasing E_{cm}, H_2^+ production with proton exchange is promoted at low collision energies.

It can also be seen from figure 2 that the cross section increases with increasing v. As the H_2 bond in a high-v state can easily be broken, this may promote the proton exchange.

Here, we should mention the effect of the rotational state j of the reactant H_2 on H_2^+ production. We have previously calculated the j effect for the reaction $H^+ + D_2$ ($v = 0$–7) $\rightarrow H + D_2^+$ with $j = 1, 5$ and 10. In [12] it has been demonstrated that the effect of the rotational state on the charge transfer (D_2^+ production) cross section is secondary to that of the v effect.

In figures 1 and 2, most of the H_2^+ ions are produced by pure charge transfer if $v \geqslant 3$ and $E_{cm} \geqslant 2$ eV. Thus, it may be interesting to investigate the isotope effect for pure charge transfer. As the vibrational level of $H_2(v = 5)$ is close to the $D_2(v = 7)$ and $T_2(v = 9)$ levels, we have calculated the cross sections with these excited molecules. The result is shown in figure 5, where the cross sections are given as a function of E_{cm}. In figure 5 the cross

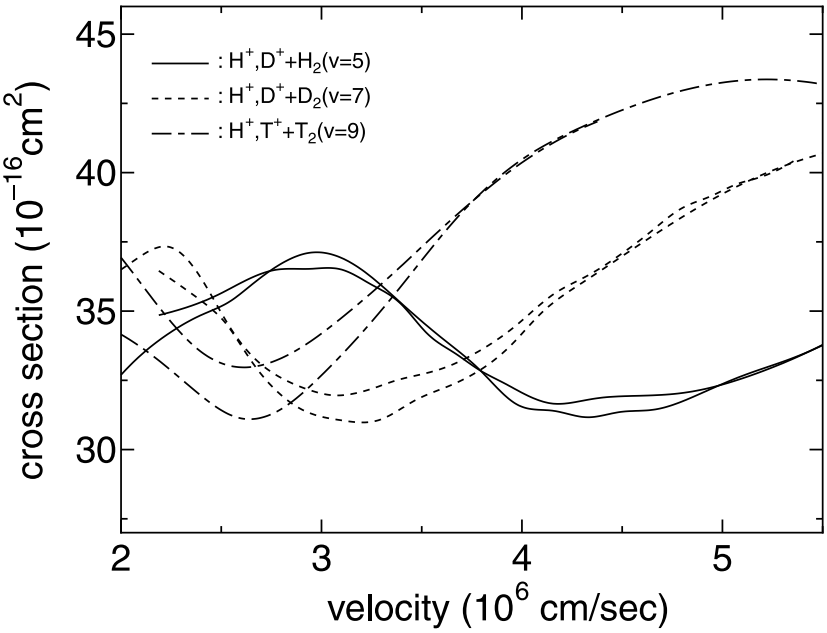

Figure 6. The collision velocity dependence of the TSH cross sections for pure charge transfer. Full curves, H^+, $D^+ + H_2$ ($v = 5$, $j = 1$); broken curves, H^+, $D^+ + D_2$ ($v = 7$, $j = 1$); chain curves, H^+, $T^+ + T_2$ ($v = 9$, $j = 1$).

sections for systems $H^+ + H_2$ ($v = 5$), $D^+ + D_2$ ($v = 7$) and $T^+ + T_2$ ($v = 9$) have similar E_{cm} dependences. However, the cross sections for other systems have very different E_{cm} dependences. As the mass of the nuclei is included in the collision energy, it may be difficult to derive a conclusion from figure 5. The isotope effect can be observed more effectively if the cross sections are given as a function of the collision velocity. Figure 6 shows the collision velocity dependence of cross sections. It can be seen from figure 6 that the cross sections for the same reactant molecule are in good agreement with each other. The cross sections are hardly affected by the substitution of incident ions H^+, D^+ or T^+. Therefore, it is expected that the charge transfer cross sections for the reaction of D^+ or T^+ with H_2 in the $3 \leqslant v \leqslant 8$ states can be derived from the present results for $H^+ + H_2$ ($3 \leqslant v \leqslant 8$), where effects of the nuclear rearrangement and dissociation are much smaller compared with the pure charge transfer.

On the other hand, it has been observed from the guided beam experiment of Schlier *et al* [14] and the present calculation that the charge transfer cross sections for the $H^+ + H_2$ ($v = 0$), $D^+ + H_2$ ($v = 0$), $H^+ + D_2$ ($v = 0$) and $D^+ + D_2$ ($v = 0$) collisions have peaks at almost the same energy of $E_{cm} = 5$ eV. Thus, if the cross sections are given as a function of velocity, the peak position is different for different isotopic combinations. This result indicates that the cross section is sensitive to the substitution of isotopes. In our calculation for $H^+ + H_2$ ($v = 0$), the H_2^+ production cross section is 1.24×10^{-16} cm^2 at 5 eV, where about half (0.56×10^{-16} cm^2) of the H_2^+ ions are produced by charge transfer with proton exchange. As the nuclear rearrangement depends on the mass of nuclei, the isotope effect is pronounced for the $v = 0$ case.

In our TSH model employed, a surface hop takes place only on the predefined avoided crossing seams ($r = 2.5\ a_0$, $R > 5.0\ a_0$). As a surface hop near the seam is not taken into account, H_2^+ production does not happen if the internuclear distance of H_2 cannot take $r \geqslant 2.5\ a_0$. Thus, it may be necessary to perform a more sophisticated calculation based

Table 2. Rate coefficients for the reaction $H^+ + H_2(v) \rightarrow H + H_2^+$. The rates were evaluated using the cross sections from the *ab initio* potential energy surfaces.

	Rate ($cm^3\ s^{-1}$)						
T (eV)	$v = 0$	1	2	3	4	5	6
$E = 0.1$ (eV)							
0.1	8.1E−22	8.7E−19	6.4E−16	2.5E−13	1.5E−09	1.5E−09	1.6E−09
0.15	2.5E−18	3.1E−16	3.2E−14	2.1E−12	1.7E−09	1.8E−09	1.9E−09
0.2	1.7E−16	6.9E−15	2.7E−13	7.1E−12	2.0E−09	2.1E−09	2.2E−09
0.3	1.4E−14	1.9E−13	2.9E−12	3.0E−11	2.4E−09	2.6E−09	2.7E−09
0.5	6.4E−13	3.5E−12	2.3E−11	1.2E−10	3.1E−09	3.5E−09	3.6E−09
0.7	3.7E−12	1.3E−11	6.0E−11	2.2E−10	3.8E−09	4.3E−09	4.4E−09
1.0	1.5E−11	3.8E−11	1.3E−10	3.8E−10	4.5E−09	5.3E−09	5.4E−09
1.5	4.8E−11	9.3E−11	2.3E−10	5.8E−10	5.4E−09	6.6E−09	6.7E−09
2.0	8.9E−11	1.5E−10	3.2E−10	7.5E−10	6.0E−09	7.7E−09	7.7E−09
3.0	1.6E−10	2.4E−10	5.0E−10	1.1E−09	7.1E−09	9.4E−09	9.4E−09
5.0	2.7E−10	4.0E−10	9.3E−10	1.8E−09	9.2E−09	1.2E−08	1.2E−08
$E = 1.0$ (eV)							
0.1	9.6E−17	1.2E−14	9.3E−13	3.0E−11	2.8E−09	3.2E−09	3.3E−09
0.15	5.6E−15	1.7E−13	4.4E−12	5.8E−11	3.0E−09	3.4E−09	3.5E−09
0.2	5.0E−14	7.5E−13	1.1E−11	9.0E−11	3.2E−09	3.5E−09	3.7E−09
0.3	5.4E−13	3.8E−12	3.0E−11	1.6E−10	3.5E−09	3.9E−09	4.1E−09
0.5	4.6E−12	1.7E−11	7.7E−11	2.8E−10	4.1E−09	4.7E−09	4.8E−09
0.7	1.3E−11	3.6E−11	1.3E−10	3.8E−10	4.5E−09	5.3E−09	5.5E−09
1.0	3.2E−11	6.9E−11	1.9E−10	5.1E−10	5.1E−09	6.2E−09	6.3E−09
1.5	7.2E−11	1.3E−10	2.9E−10	6.9E−10	5.8E−09	7.3E−09	7.4E−09
2.0	1.1E−10	1.8E−10	3.7E−10	8.4E−10	6.4E−09	8.3E−09	8.3E−09
3.0	1.8E−10	2.7E−10	5.5E−10	1.2E−09	7.4E−09	9.8E−09	9.8E−09
5.0	2.8E−10	4.2E−10	1.0E−09	2.0E−09	9.5E−09	1.2E−08	1.2E−08
$E = 5.0$ (eV)							
0.1	1.7E−11	8.6E−11	3.6E−10	9.0E−10	6.7E−09	8.0E−09	8.3E−09
0.15	2.7E−11	1.0E−10	3.6E−10	8.9E−10	6.7E−09	8.1E−09	8.3E−09
0.2	3.6E−11	1.1E−10	3.6E−10	8.9E−10	6.6E−09	8.2E−09	8.4E−09
0.3	5.4E−11	1.3E−10	3.7E−10	8.9E−10	6.6E−09	8.4E−09	8.5E−09
0.5	8.4E−11	1.6E−10	3.9E−10	8.9E−10	6.6E−09	8.6E−09	8.6E−09
0.7	1.1E−10	1.9E−10	4.1E−10	9.1E−10	6.7E−09	8.9E−09	8.8E−09
1.0	1.4E−10	2.2E−10	4.4E−10	9.6E−10	6.9E−09	9.2E−09	9.2E−09
1.5	1.8E−10	2.6E−10	5.1E−10	1.1E−09	7.3E−09	9.8E−09	9.7E−09
2.0	2.1E−10	3.0E−10	6.0E−10	1.3E−09	7.8E−09	1.0E−08	1.0E−08
3.0	2.6E−10	3.7E−10	8.2E−10	1.7E−09	8.8E−09	1.2E−08	1.2E−08
5.0	3.2E−10	5.2E−10	1.3E−09	2.5E−09	1.1E−08	1.4E−08	1.4E−08

on the fewest switch method of Tully [30], which allows transitions to occur at any place where the electronic coupling is significant, not just at localized avoided crossings. Moreover, to overcome the limitations of the classical method, quantum mechanical calculations may be required. Baer and Nakamura have reported that the microscopic reversibility cannot be fulfilled within classical mechanics and that large uncertainties should be included in cross sections for low collision energies [31]. Quantum effects such as tunnelling also cannot be treated in the classical calculation. Therefore, an accumulation of the theoretical calculations as well as experimental data is strongly required.

Finally, we give the Maxwellian-averaged rate coefficient for the reaction $H^+ + H_2$ ($v = 0$–14) $\rightarrow H + H_2^+$. The rate coefficients have been estimated from the cross section data given in

Table 3. Rate coefficients for the reaction $H^+ + H_2(v) \rightarrow H + H_2^+$. The rates were evaluated using the cross sections from the diatomics-in-molecules potential surfaces.

	Rate ($cm^3\ s^{-1}$)							
T (eV)	$v = 7$	8	9	10	11	12	13	14
$E = 0.1$ (eV)								
0.1	1.8E−09	1.8E−09	1.9E−09	1.7E−09	1.6E−09	1.5E−09	1.4E−09	1.4E−09
0.15	2.1E−09	2.1E−09	2.1E−09	2.0E−09	1.8E−09	1.7E−09	1.6E−09	1.5E−09
0.2	2.4E−09	2.4E−09	2.4E−09	2.2E−09	2.0E−09	1.9E−09	1.7E−09	1.5E−09
0.3	2.9E−09	2.9E−09	2.8E−09	2.6E−09	2.3E−09	2.1E−09	1.9E−09	1.6E−09
0.5	3.8E−09	3.7E−09	3.5E−09	3.2E−09	2.7E−09	2.4E−09	2.0E−09	1.6E−09
0.7	4.5E−09	4.4E−09	4.0E−09	3.5E−09	3.0E−09	2.5E−09	2.0E−09	1.6E−09
1.0	5.4E−09	5.1E−09	4.6E−09	4.0E−09	3.3E−09	2.7E−09	2.0E−09	1.6E−09
1.5	6.4E−09	6.0E−09	5.3E−09	4.5E−09	3.7E−09	2.9E−09	2.1E−09	1.6E−09
2.0	7.3E−09	6.7E−09	5.9E−09	5.0E−09	4.0E−09	3.0E−09	2.1E−09	1.6E−09
3.0	8.7E−09	8.0E−09	7.0E−09	5.9E−09	4.6E−09	3.3E−09	2.3E−09	1.6E−09
5.0	1.1E−08	1.0E−08	8.8E−09	7.2E−09	5.4E−09	3.9E−09	2.6E−09	1.8E−09
$E = 1.0$ (eV)								
0.1	3.5E−09	3.5E−09	3.4E−09	3.1E−09	2.7E−09	2.4E−09	2.1E−09	1.7E−09
0.15	3.7E−09	3.7E−09	3.5E−09	3.2E−09	2.8E−09	2.4E−09	2.1E−09	1.7E−09
0.2	3.8E−09	3.8E−09	3.7E−09	3.3E−09	2.8E−09	2.5E−09	2.1E−09	1.7E−09
0.3	4.2E−09	4.2E−09	3.9E−09	3.5E−09	3.0E−09	2.5E−09	2.0E−09	1.6E−09
0.5	4.9E−09	4.7E−09	4.3E−09	3.8E−09	3.2E−09	2.6E−09	2.0E−09	1.6E−09
0.7	5.4E−09	5.2E−09	4.6E−09	4.0E−09	3.3E−09	2.7E−09	2.0E−09	1.6E−09
1.0	6.1E−09	5.7E−09	5.1E−09	4.3E−09	3.6E−09	2.8E−09	2.1E−09	1.6E−09
1.5	7.0E−09	6.5E−09	5.7E−09	4.8E−09	3.9E−09	3.0E−09	2.1E−09	1.6E−09
2.0	7.7E−09	7.1E−09	6.2E−09	5.3E−09	4.2E−09	3.1E−09	2.2E−09	1.6E−09
3.0	9.1E−09	8.4E−09	7.3E−09	6.1E−09	4.7E−09	3.4E−09	2.3E−09	1.6E−09
5.0	1.1E−08	1.0E−08	9.0E−09	7.4E−09	5.6E−09	4.0E−09	2.6E−09	1.8E−09
$E = 5.0$ (eV)								
0.1	7.9E−09	7.2E−09	6.0E−09	4.9E−09	4.0E−09	2.9E−09	2.0E−09	1.4E−09
0.15	7.9E−09	7.1E−09	6.0E−09	5.0E−09	4.0E−09	2.9E−09	2.0E−09	1.4E−09
0.2	7.9E−09	7.1E−09	6.0E−09	5.0E−09	4.0E−09	3.0E−09	2.0E−09	1.5E−09
0.3	7.9E−09	7.1E−09	6.1E−09	5.1E−09	4.1E−09	3.0E−09	2.1E−09	1.5E−09
0.5	8.0E−09	7.2E−09	6.2E−09	5.3E−09	4.2E−09	3.1E−09	2.1E−09	1.5E−09
0.7	8.2E−09	7.4E−09	6.4E−09	5.4E−09	4.3E−09	3.2E−09	2.1E−09	1.5E−09
1.0	8.4E−09	7.7E−09	6.7E−09	5.7E−09	4.4E−09	3.3E−09	2.2E−09	1.5E−09
1.5	9.0E−09	8.2E−09	7.2E−09	6.0E−09	4.7E−09	3.4E−09	2.3E−09	1.6E−09
2.0	9.6E−09	8.8E−09	7.7E−09	6.4E−09	4.9E−09	3.6E−09	2.4E−09	1.6E−09
3.0	1.1E−08	9.9E−09	8.5E−09	7.0E−09	5.3E−09	3.8E−09	2.5E−09	1.7E−09
5.0	1.3E−08	1.2E−08	1.0E−08	8.1E−09	6.0E−09	4.3E−09	2.8E−09	1.9E−09

figure 1. The results are shown in tables 2 and 3. The rates are expressed as functions of the plasma temperature T and the H_2 temperature E. From comparison of the TSH results with the experimental and quantum mechanical results in section 2, the uncertainties in rates for $v = 0$ are estimated to be a factor of 0.5 to 2, and similar uncertainties may be included for $v > 0$.

4. Summary

The cross sections for the reaction $H^+ + H_2$ ($v = 0$–14) $\rightarrow$ $H_2^+ + H$ have been calculated in the centre-of-mass collision energy range of $E_{cm} \leqslant 20.0$ eV by employing the TSH method. The

obtained cross sections for $v \leqslant 5$ increase rapidly with increasing v. For $v \geqslant 3$, most H_2^+ ions are produced by pure charge transfer, and charge transfer accompanied by proton exchange is significant only for the low-energy region of $E_{cm} < 2$ eV. The cross sections for $v = 5, 6$ have almost the same values and those for $v > 6$ decrease with increasing v. The enhanced H_2^+ production for $v \leqslant 5$ has been explained using the features of PESs. The decrease in H_2^+ production for high-v states has been attributed to increasing dissociation and the features of the TSH model with the Landau–Zener formula. The isotope effect has been discussed with a limited number of TSH calculations and it has been pointed out that the charge transfer cross sections are almost independent of the substitution of incident ions if the reaction is dominated by pure charge transfer. The uncertainties arising in the present calculation have been discussed and it has been pointed out that cross sections include more uncertainties near the threshold. The rate coefficients have been estimated from the cross sections in the range ($0.1 \leqslant E \leqslant 5.0$ eV, $0.1 \leqslant T \leqslant 5.0$ eV).

References

[1] Holliday M G, Muckerman J T and Friedman L 1971 *J. Chem. Phys.* **54** 1058
[2] Maier W B II 1971 *J. Chem. Phys.* **54** 2732
[3] Krenos J R, Preston R K, Wolfgang R and Tully J C 1974 *J. Chem. Phys.* **60** 1634
[4] Last I, Gilibert M and Baer M 1997 *J. Chem. Phys.* **107** 1451 and related references therein
[5] Niedner G, Noll M, Toennies J P and Schlier Ch 1987 *J. Chem. Phys.* **87** 2685
[6] Baer M, Schatteburg G N and Toennies J P 1989 *J. Chem. Phys.* **91** 4169
[7] Janev R K 1995 *Atomic and Molecular Processes in Fusion Edge Plasmas* ed R K Janev (New York: Plenum) p 1
[8] Post D E 1995 *J. Nucl. Mater.* **220–2** 143
[9] Krasheninnikov S I, Pigarov A Yu and Sigmar D J 1996 *Phys. Lett.* A **214** 285
[10] Janev R K 1998 *Contrib. Plasma Phys.* **38** 307
[11] Ichihara A, Shirai T and Yokoyama K 1996 *J. Chem. Phys.* **105** 1857
[12] Ichihara A, Iwamoto O and Yokoyama K 2000 *Atom. Plasma-Mater. Int. Data Fusion.* **9** at press
[13] Ochs G and Teloy E 1974 *J. Chem. Phys.* **61** 4930
[14] Schlier Ch, Nowotny U and Teloy E 1987 *Chem. Phys.* **111** 401
[15] Chapman S 1992 *Adv. Chem. Phys.* **82** 423
[16] Tully J C and Preston R K 1971 *J. Chem. Phys.* **55** 562
[17] Karplus M, Porter R N and Sharma R D 1965 *J. Chem. Phys.* **43** 3259
[18] Blais N C and Truhlar D G 1976 *J. Chem. Phys.* **65** 5335
[19] Janev R K, Langer W D, Evans K Jr and Post D E Jr 1987 *Elementary Processes in Hydrogen–Helium Plasmas* (Berlin: Springer)
[20] Landau L D 1932 *Phys. Z. Sow.* **2** 46
[21] Zener C 1932 *Proc. R. Soc.* A **137** 696
[22] Stuckelberg E C G 1932 *Helv. Phys. Acta* **5** 369
[23] Zhu C and Nakamura H 1995 *J. Chem. Phys.* **102** 7448
[24] Nakamura H and Zhu C 1996 *Comment. At. Mol. Phys.* **32** 249
[25] Ichihara A and Yokoyama K 1995 *J. Chem. Phys.* **103** 2109
[26] Ellison F O 1963 *J. Am. Chem. Soc.* **85** 3540–4
[27] Gealy M W and Van Zyl B 1987 *Phys. Rev.* A **36** 3091
[28] Baer M 1992 *Adv. Chem. Phys.* **82** 187
[29] Bauschlicher C W Jr, O'Neil S V, Preston R K, Schaefer H F III and Bender C F 1973 *J. Chem. Phys.* **59** 1286
[30] Tully J C 1990 *J. Chem. Phys.* **93** 1061
[31] Baer M and Nakamura H 1987 *J. Chem. Phys.* **87** 4651